Synthesis of titanium oxide nanoparticles using DNA-complex as template for solution-processable hybrid dielectric composites

Accepted Manuscript

Synthesis of Titanium Oxide Nanoparticles Using DNA-Complex as Template for Solution- Processable Hybrid Dielectric Composites

J.C. Ramos, I. Mejia, J. Murphy, M. Quevedo, P. Garcia, C.A. Martinez

Synthesis of Titanium Oxide Nanoparticles Using DNA-Complex as Template for Solution- Processable Hybrid Dielectric Composites.

J.C. Ramos[a], I. Mejia[b], J. Murphy[b], M. Quevedo[b], P. Garcia[c] and C.A. Martinez[c].

a. Center for Sustainable Materials Chemistry, 153 Gilbert Hall, Oregon State University, Corvallis, Oregon, USA. Phone +1(541)-737-2081.

b. Department of Materials Science and Engineering, University of Texas at Dallas, Dallas, Texas, USA. Phone: +1(972) 883-5714.

c. Engineering and Technology Institute, Autonomous University of Ciudad Juarez, Ciudad Juarez, Chihuahua, Mexico. +52(656)688-4800.

Abstract

We report the synthesis of TiO_2 nanoparticles prepared by the hydrolysis of titanium isopropoxide (TTIP) in the presence of a DNA complex for solution processable dielectric composites. The nanoparticles were incorporated as fillers in polycarbonate at low concentrations (1.5, 5 and 7 wt%) to produce hybrid dielectric films with dielectric constant higher than thermally grown silicon oxide. It was found that the DNA complex plays an important role as capping agent in the formation and suspension stability of nanocrystalline anatase phase TiO_2 at room temperature with uniform size (~6 nm) and narrow distribution. The effective dielectric constant of spin-cast polycarbonate thin-films increased from 2.84 to 13.43 with the incorporation of TiO_2 nanoparticles into the polymer host. These composites can be solution processed with a maximum temperature of 90 ℃ and could be potential candidates for its application in low-cost macro-electronics.

Keywords: TiO_2, DNA, hybrid nanocomposite, dielectric constant, solution processed, macro-electronics

1. Introduction

In the field of electronics, there has been an increasing interest over the last few years in the development of the low cost macro-electronics area. For the successful development of this technology, not only semiconductor materials, but also dielectric materials are required to be solution processable. Those dielectrics, however, need to perform in an acceptable way to be introduced in real applications. They should be able to provide a low leakage current, high capacitance to enable low voltage operation, and uniform and smooth surface. Ceramics such as TiO_2 are candidates for dielectric materials because of their large band-gap and high dielectric constants [1,2]. Films of

these oxides, however, are brittle and require high temperature processing, which makes the technology quite expensive an incompatible with flexible substrates. In contrast, polymers such as poly(4-vinylphenol) [3], polyimide [4], polymethylmetacrylate (PMMA) [5], polycarbonate (PC) [6] and polyvinylalcohol (PVA) [7], have been used as gate dielectrics as an alternative to vacuum deposited insulators. These polymers can be processed at low temperatures, but their dielectric constants are low compared to those of ceramic films [8]. Inorganic oxide-polymer composites combine the processing flexibility of polymers and the high dielectric constant of ceramics [8,9]. Previous studies have demonstrated that the use of TiO_2 in a polymer matrix can increase its dielectric constant [10,11]. However, the results show poor performance due to aggregation and sedimentation of the nanoparticles caused by their high surface energy, yielding a non-uniform dispersion. On the other hand, to produce and stabilize TiO_2 nanoparticles in composites, complicated systems such as milling or in-situ synthesis are used [12,13]. Nevertheless, these systems do not provide small and uniform particle size, limiting the thickness of the overall film to avoid pin-holes and discontinuities which impact negatively the performance of the electronic devices.

Uniform small TiO_2 nanoparticles that can be stable in a polymer solution and film would improve the aforementioned limitations [14]. Furthermore, a smooth composite film could be thinned without introducing pin-holes in the film. In order to obtain TiO_2 nanoparticles homogeneously dispersed in a host polymer, the control of several parameters is required such as size, shape, surface and self-assemble properties [15,16]. It is also desirable to use a simple and scalable synthesis method, ideally one with low cost and toxicity. Several methods for the synthesis of TiO_2 nanoparticles have been reported such as hydrothermal [17], sonication assisted [18], and sol-gel among others [19]. Sol-gel is one of the most widely applied approaches for the preparation of nano-sized metal oxides. However, the experimental results have shown that uncontrolled sol-gel reactions can lack stability or size and shape uniformity due to the condensation reaction involved in the hydrolysis of the TiO_2 precursors, which take place in random locations in an amorphous polymer matrix [20]. On the other hand, deoxyribonucleic acid (DNA) is a well-known nanostructured material that, beyond its biological function, has been utilized for directing the assembly of various artificial

nanostructures [19, 21]. Besides the use of DNA as template for synthesis of nanomaterials, this molecule has been extensively studied for its electronic properties and potential application in nanoelectronics [22]. However the study of its electrical properties is out of the specific aims of this research.

PC is a well-known dielectric polymer, soluble in non-polar solvents, so it does not absorb water. This is an important factor to reduce the leakage current. PC has been reported previously as a promising host polymer and it was chosen as the polymer host for this study [8]. In this context, the present work describes, for the first time, the preparation and characterization of TiO_2 nanoparticles by means of a modified sol-gel process using hexadecyltrimethyl ammonium bromide (CTAB) and DNA complex as template to control the particle size, shape and its size distribution, and provides solubility in alcohols. This could help to overcome some of the problems discussed above and create homogeneous hybrid composite films with desirable dielectric properties using solution processes at low temperature.

2. Materials and Methods.

The DNA/CTAB complex was prepared using a similar methodology to that developed by Heckman *et al*. [23]. An aqueous solution (4 g/L) of DNA (Acros Organics) was prepared under vigorous stirring until it was completely dissolved. Later, the DNA solution was added drop-wise to an aqueous solution of CTAB ($C_{19}H_{42}BrN$) (Sigma-Aldrich) (4 g/L) with vigorous stirring. The DNA/CTAB complex precipitated, as the DNA was added. The solution was kept under agitation for 4 h at room temperature. The mixture was filtered through a 1 μm pore size Teflon membrane to recover the organic complex and washed with deionized water. The precipitate was then collected and dried in a rotavapor for 4 h at 40 °C and stored at 4 °C until its use. TiO_2 nanoparticles were prepared by drop-wise addition of a 6.6 mmol solution of titanium (IV) isopropoxide ($Ti(OPri)_4$), (99.999%, Sigma-Aldrich), (TIIP), to 6 mL of an homogeneous DNA/CTAB-isopropanol solution (7 g/L) (solution 1) under vigorous magnetic agitation for 4 h at ~25 °C. After this, the solution was kept stirring for another 2 h to ensure a homogeneous solution. Then, 50 mL of an aqueous solution at pH 2 (previously adjusted with HNO_3 and NH_4OH) (solution 2) was used as the hydrolysis catalyst by adding it dropwise to

solution 1 with vigorous stirring; a precipitate was obtained after 20 h. The precipitate was washed with deionized water and centrifuged at 10,000 rpm for 5 min, then re-suspended in methanol. PC was dissolved in chlorobenzene (9 wt%) and blended with different concentrations of TiO_2/ DNA/CTAB dispersions (1.5, 5 and 7 wt%) with an ultrasonic horn. To fabricate metal-insulator-metal (MIM) devices, the composite solutions were spin coated at 2000 rpm for 20 sec to produce ~100 nm thick films onto silicon (Si) wafers (100) coated with 100 nm of Au (bottom contact), and then dried in air at 90 °C for 60 min. Finally, Au was thermally evaporated through a shadow mask to produce circular electrodes with different dimensions (diameter ranged from 50 to 500 μm) as top contacts. The physicochemical characterization of nanoparticles was performed by means of Fourier transform infrared (FTIR) spectroscopy using a Nicolet 6700 spectrophotometer (Thermoscientific). The UV-Vis absorption spectra were obtained with a USB 4000 Ocean Optics photodetector. X-ray diffraction (XRD) patterns were analyzed in a X'Pert PRO (PANalytical) diffractometer using CuKα radiation at 40 kV and 50 mA with a scanning speed of 0.02°/min at 2θ steps. A JEOL 2200FS high resolution field emission transmission electronic microscope (HR-FE-TEM) was also used for morphology characterization, while the thickness of the films was measured using a DekTak profilometer. Electrical characterization was done by current-voltage (I-V), capacitance-voltage (C-V) and capacitance-frequency (C-F) measurements using MIM devices applying an electric field in the range of -0.5 to 0.5 MV/cm at room temperature in air atmosphere using a 4200 Keithley characterization system under dark conditions.

3. Results and discussion.

The goal of developing this synthesis method was to obtain crystalline TiO_2 nanoparticles with small size and uniform size distribution that could be deposited via solution processes using processing temperatures compatible with flexible electronic technologies. Tailoring the nanoparticle surface during the synthesis with DNA/ complex resulted in stable suspensions in short carbonated chain alcohols or dimethylformamide for more than five days, which is a main requirement to introduce them as nanofillers in the organic hosts. In comparison, we tested commercial TiO_2 nanoparticles, which precipitated immediately in any of these solvents. FTIR spectra of the DNA/CTAB

complex used for the synthesis of the nanoparticles (Figure 1a) exhibit a band from 1670 to 1636 cm^{-1}, which is attributed to the C=C stretching vibrations of the thymine and adenine and N-H bending vibrations of guanine from the DNA molecule. The signal at 1470 cm^{-1} shows stretching vibrations of CH_2, due to the CTAB molecule. The bands around 1341 cm^{-1}, correspond to a C-C-H chain deformation band of the CTAB. The FTIR spectrum of the synthetized TiO_2 nanoparticles is also shown and the same signals attributed to the DNA/CTAB are observed. This proves that the organic complex is still present on the nanoparticles even after the purification treatments, providing a way to disperse and stabilize them in suspensions. The spectra also suggest that the TiO_2 strongly interacts with the organic complex because the signal attributed to the C-C-H of CTAB (1341 cm^{-1}) shows chain scissoring, while the signal at 1470 cm^{-1} is almost reduced to plane, also, the signals attributed to the DNA molecule in the complex suffer a small shifting to lower wavenumbers when interacting with TiO_2. Other major feature of the FTIR spectrum is a broad and intense band below 1000 cm^{-1} assigned to Ti-O-Ti bond vibrations of the metal oxide particles.

UV-Vis spectra of the DNA/CTAB complex and TiO_2 nanoparticles are shown in Figure 1b. The DNA/CTAB exhibited the maximum absorption at approximately 260 nm, identically to the natural DNA owed to the alternating single and double bonds of aromatic nitrogenous bases [24]. In contrast, when observing the spectral behavior of TiO_2 nanoparticles, the absorbance is low between 600 to 500 nm with a gradual increment near the Tauc region. This is due to the charge-transfer from the valence band ($2p$ orbitals of the oxide anions) to the conduction band ($3d$ of the Ti cations) [25]. The optical band-gap (E_g) of the TiO_2 nanoparticles has been calculated by plotting the energy over the optical density versus the energy in eV and extrapolating the straight line portion of the curve to intercept the energy axis. The nanoparticles show an indirect type E_g estimated to be 3.66 eV. This value is larger than expected for anatase phase (~3.22 eV) [26]. A quantum size effect for the nanoparticles seems to be observed, and this differs from a previous report that suggests the size of a TiO_2 nanoparticle should be 1.5 nm or less in order to show quantum size effects [27]. This discrepancy may be due to the fact that, in our case, the TiO_2 nanoparticles are mostly separated in suspension without large agglomerates. This observation is consistent with the

crystallite sizes obtained from XRD patterns and with previous reported works [16]. Other important differences between TiO_2 nanoparticles spectra and the DNA/CTAB spectra are the bathochromic shift and the absorbance ratio between 240 and 260 nm. This shift in the absorbance on the metal-to-ligand charge transfer (MLCT) band is indicative of the strong interaction via groove binding between TiO_2 nanoparticles and DNA/CTAB complex, which is supported by FTIR results and previous reported works [28].

XRD studies of the TiO_2 nanoparticles were performed in order to verify that the titanium oxide formation took place under the reaction conditions employed and to elucidate its crystal phase. Figure 2 shows the XRD pattern for TiO_2 nanoparticles. This pattern exhibits peaks at 25.4°, 37.8°, 48.1°, 54.4°, 62.8°, 68.9°, 70.1°, 75.3°, 82.8° and 94.8°, which correspond to the (101), (004), (200), (105), (204), (116), (220), (215), (224) and (305) lattice planes of the tetragonal structure of anatase phase, respectively. Also a small and broad peak appears at 30.6°, which could be assigned to the (121) Miller index of orthorhombic brookite, present in the sample in small amounts. The compound identification and crystal analysis was obtained through the X´Pert High-Score Plus software, and is in agreement with the JCPDS XRD spectra data (JCPDS No. 84-1286, 73-1764 and 21-1272). These results show that highly crystalline nanoparticles can be obtained despite the low reaction temperature (~25 °C). This is a notable feature because in most cases sol-gel processes lead to amorphous materials, and subsequent annealing is necessary to induce crystallization [29,30]. Obtaining crystalline TiO_2 improves dielectric performance over the amorphous phase because of their theoretical dielectric constants of 40 and 27, respectively [8]. The calculated average crystallite size was 5.9 nm, using Scherrer's equation [31] by peak-broadening analysis of (101) and (004) XRD signals of anatase. The interplanar distances (*d*) were calculated by cell refinement for anatase phase giving $a=b=$ 0.35 nm and $c=$ 1.18 nm and a cell volume of 0.473 nm^3. The lattice parameter in *a* and *b* are smaller and *c* larger in comparison with the JCPDS values (JCPDS No. 21-1272, $a=0.37852$ nm and $c=0.95139$ nm). This effect suggests displacement of atoms from their ideal sites when TiO_2 becomes nanocrystalline, as reported before [32].

The distribution of particle size, crystallinity, and morphology of the nanoparticles was studied by HRTEM in order to achieve consistent and accurate measurement (Figure 3). In the micrograph of Figure 3a, we can observe well distributed nanoparticles with uniform size and shape. The average nanoparticle size was calculated according to sampling theory by the analysis of 100 nanoparticles giving a mean particle diameter of 5.97 nm with a standard deviation of 1.08 nm (inset graph in Figure 3a). The results are in good agreement with those obtained from XRD for crystallite size but they differ from those obtained by other authors where they used only CTAB as a capping agent [33], demonstrating the DNA effect in the organic complex to control the size and shape of the nanoparticles. The element composition of the nanoparticles was confirmed by energy dispersive X-ray (EDS) spectroscopy analysis under TEM (Figure 3b). EDS point spectrum taken from an area highly loaded with nanoparticles showed strong O and Ti signals from TiO_2 with an atomic ratio of 2.6. The excess in oxygen could be due to the presence of adsorbed oxygen as well as the oxygen coming from the bases and phosphate groups in the DNA/CTAB, as is expected because of the presence of phosphorus, carbon and nitrogen traces in the sample. These observations confirmed the results obtained by FTIR. The crystallinity of the nanoparticles was confirmed by the selected area electron diffraction (SAED) pattern (Figure 3c). It showed well resolved bright polymorphic ring patterns, typical for the anatase phase corresponding to the planes (101), (004), (200) and (105). These patterns were in agreement with the XRD results in Figure 2. The fringes of the TiO_2 nanoparticles were used to determine the crystallographic spacings and their orientation. Figure 3d gives an additional evidence of nanoparticles crystallinity showing an HRTEM micrograph of anatase nanocrystallites consisting of tetragonal particles with crystal lattice planes with a *d* spacing of 0.35 nm. The fringes corresponding to the (101) crystallographic planes of anatase were the most prominent.

To investigate the electrical effects of introducing TiO_2 nanoparticles into a host polymer (polycarbonate), capacitance-voltage (C-V) were performed at 1MHz in the MIM devices (Figure 4a). The capacitance density of the TiO_2-PC films was higher than that of the pristine PC dielectric layer and it increased remarkably with the increase in nanoparticle content, because of the higher dielectric constant of TiO_2. In Figure 4b, the dielectric

analysis of capacitance-frequency is presented. Here, same trend as C-V is observed at low frequencies, however, we observe that near $1x10^4$ Hz, capacitances abruptly decrease and dielectric relaxation occurs. This relaxation at lower frequency is more evident as nanoparticle content increases due to more TiO_2 powder effect in the organic matrix, as observed before [34]. Above $5x10^5$ Hz, the capacitances become more stable and a slight reduction is observed along further frequencies.

From the previous graphs, dielectric constants were calculated using: $C = \varepsilon_0\varepsilon/x_0$, where C is the capacitance per unit area at 1 mHz, ε_0 is the vacuum permittivity, ε is the dielectric constant and x_0 is the dielectric thickness. The relative dielectric constant of the neat polymer is 2.84 which is close to the value reported earlier [35]. And this increases as the amount of nanoparticles in the composite increases as well from 3.22 for 1.5 wt%, to 8.42 for 5 wt%, and 13.43 for 7 wt%, which represents an increase of 4.6 times in comparison with that of the pristine PC. This increment is larger than those compared with previously reported TiO_2 nanocomposites for a given percentage of filler [36]. The experimental dielectric constant of the composite with 1.5 wt% of TiO_2 is close to the values theoretically obtained by the volume-fraction average model, Maxwell equation and Bruggerman model [39] using a theoretical dielectric constant of 2.9 for the pristine PC and 40 for anatase TiO_2 according to reported values [8]. However, the experimental values obtained from devices with higher TiO_2 content does not follow the same trend of the calculated models (Figure 4c). This could be due to the simple composite medium theories used, which do not take into account the influence of the inter-particle dipolar interactions or their effect on the surrounding medium. Another factor that could affect the measured dielectric constant is the nanoparticles size effect, as observed previously [37]. Percolation theory and the self-consistent effective medium theory (SC-EMT) have been used to model the dielectric properties of hybrid nanocomposites [38], similar to those studied in this work. They have obtained, theoretically, a behavior similar to what we experimentally obtained here, attributing the giant increase in the dielectric constant to the percolation phenomenon.

The leakage current of the polycarbonate insulator at 0.5 MV/cm was $\sim 1x10^{-8}$ A/cm^2, due to its dense chemical structure and covalent bonds. The leakage current of the 1.5 wt% TiO^2 sample was $\sim 3.4x10^{-8}$ A/cm^2, which was almost the same as that of the

pristine PC insulator. It was observed that the current flow through the devices with higher nanoparticles load increased with increasing nanoparticle load: at 0.5 MV/cm the leakage current increased by 2 orders of magnitude for 5% and 5 orders for 7% load. Although, below 0.25 MV/cm, the currents were lower enough for usual operational thin film transistors, with a maximum of ~1.2×10^{-6} A/cm^2 for the 7% loaded composite as showed in Figure 4d. This increase in the leakage current when a polymer matrix is loaded with inorganic filler has been observed before [39]. An explanation has been proposed before with an interfacial transition model that considers a free volume or void layer at the transition between the host and filler. This could create low dielectric permittivity zones that could trigger localized discharge causing free carrier movement [9]. Even if these leakage currents increase, those values could be reduced by the integration of electrodes with a higher work function, such as Ru or Pt, as found in previous works [40].

4. Conclusions.

In the present work we developed a facile modified sol-gel technique performed at room temperature for the preparation of suspension stable TiO$_2$ nanoparticles (~6 nm diameter) with crystalline anatase phase at room temperature. It was found that the DNA/CTAB complex plays a key role in the formation of the crystalline phase, the size, and suspension stability of TiO$_2$ nanoparticles. We combined the material crystallinity with a tailorable surface, promoting better dispersion of the nanoparticles in the polymer. The particles have been incorporated as fillers into a polycarbonate matrix in order to increase the effective dielectric constant of composites. The presence of TiO$_2$ nanoparticles enhanced the effective dielectric constant of the composites. The dielectric constant of the films increased when the TiO$_2$ content increases, reaching a value of 13.43 with 7 wt% of TiO$_2$, which was around 4.6 times larger than that of the pristine PC. The leakage currents also increased as the TiO$_2$ amount increased; however, the composites could sufficiently suppress leakage currents and be used in low-voltage conditions, such as 3 V. This method offers an economical way to fabricate hybrid nanocomposites as insulators with high capacitance without the aforementioned complications associated with inorganic high dielectric constant materials. This also provides the opportunity to tune the dielectric constant. The composites can be used in

solution processes with a maximum processing temperature of 90 ℃, which enables their use in low-cost, flexible electronics.

Figures foot notes.
Figure 1. a) FTIR spectra of TiO_2 nanoparticles and the DNA/CTAB complex. b) UV-Vis absorbance spectra of TiO_2 nanoparticles and DNA/CTAB complex, inset figure corresponds to the energy calculations for absorption edge analysis.

Figure 2. XRD patterns of TiO_2 nanoparticles. The peak labels correspond to the Miller indices of the crystal planes.

Figure 3. HR-TEM characterization of TiO_2 nanoparticles. a) bright field image, inserted figure corresponds to the size distribution analysis. b) elemental analysis by EDS under TEM. c) SAED pattern, and d) HR-TEM micrograph at higher magnification and filtered lattice.

Figure 4. Electrical characterization of TiO_2 nanoparticles-polycarbonate composites with different filler loading. a) Capacitance density vs. applied electric field. b) Frequency response of dielectric composites. c) Effect of TiO_2 nanoparticles in the dielectric constant at different ratios, experimental and theoretical values. d) Current density vs. applied electric field.
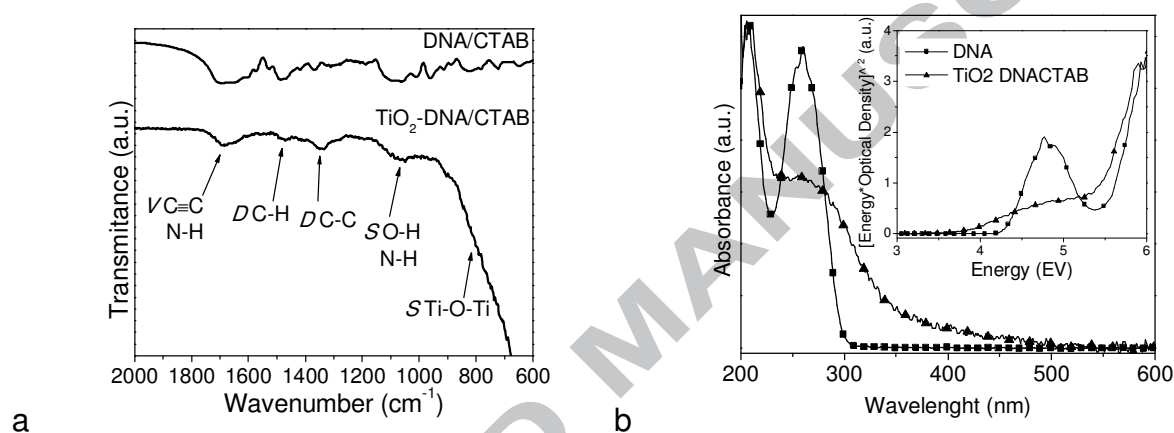
Figures.

a
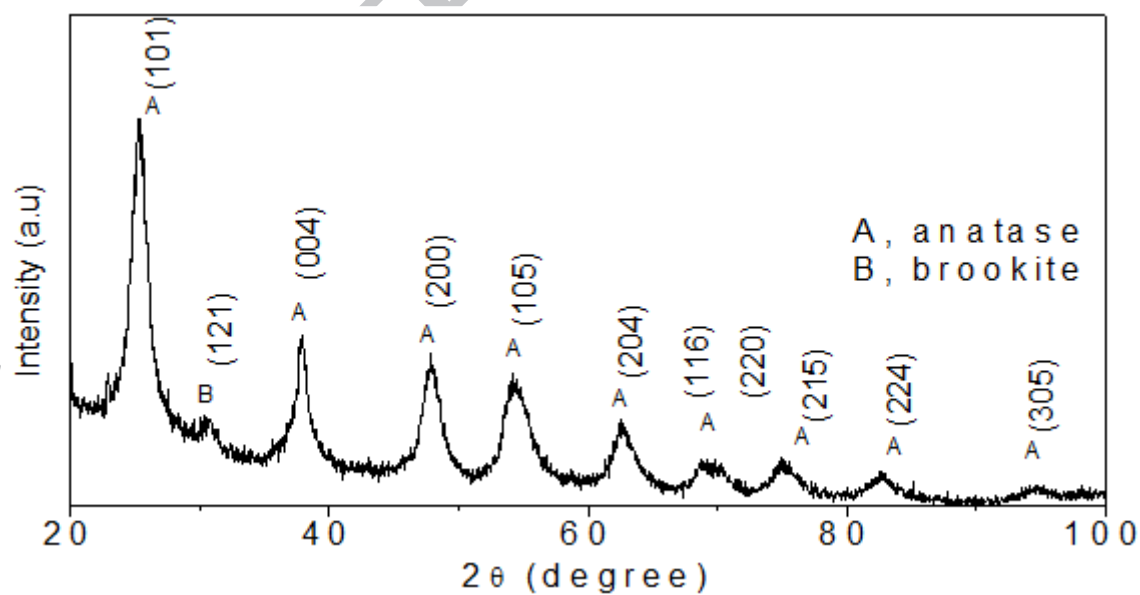

b

Figure 1.

Figure 2.

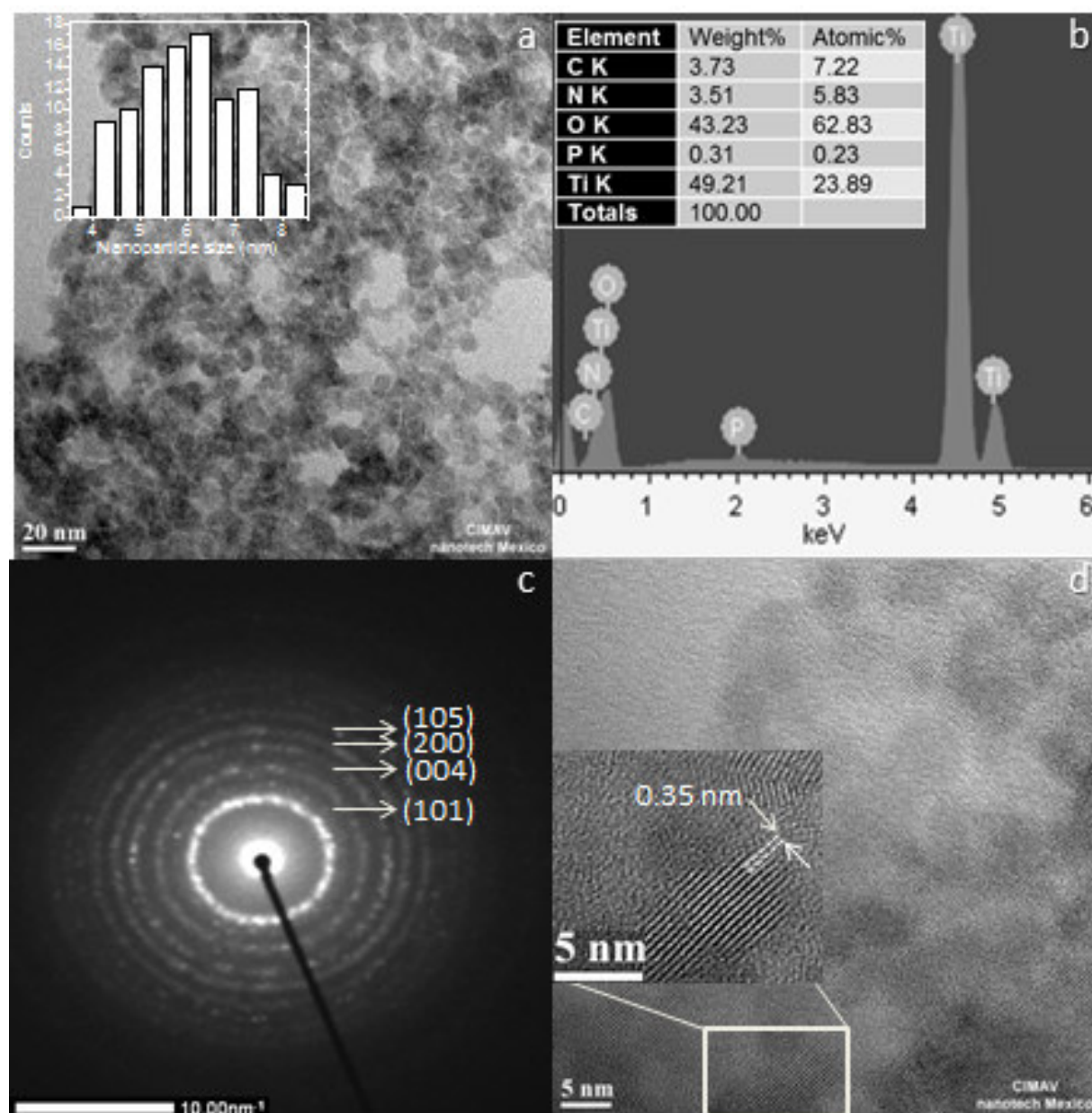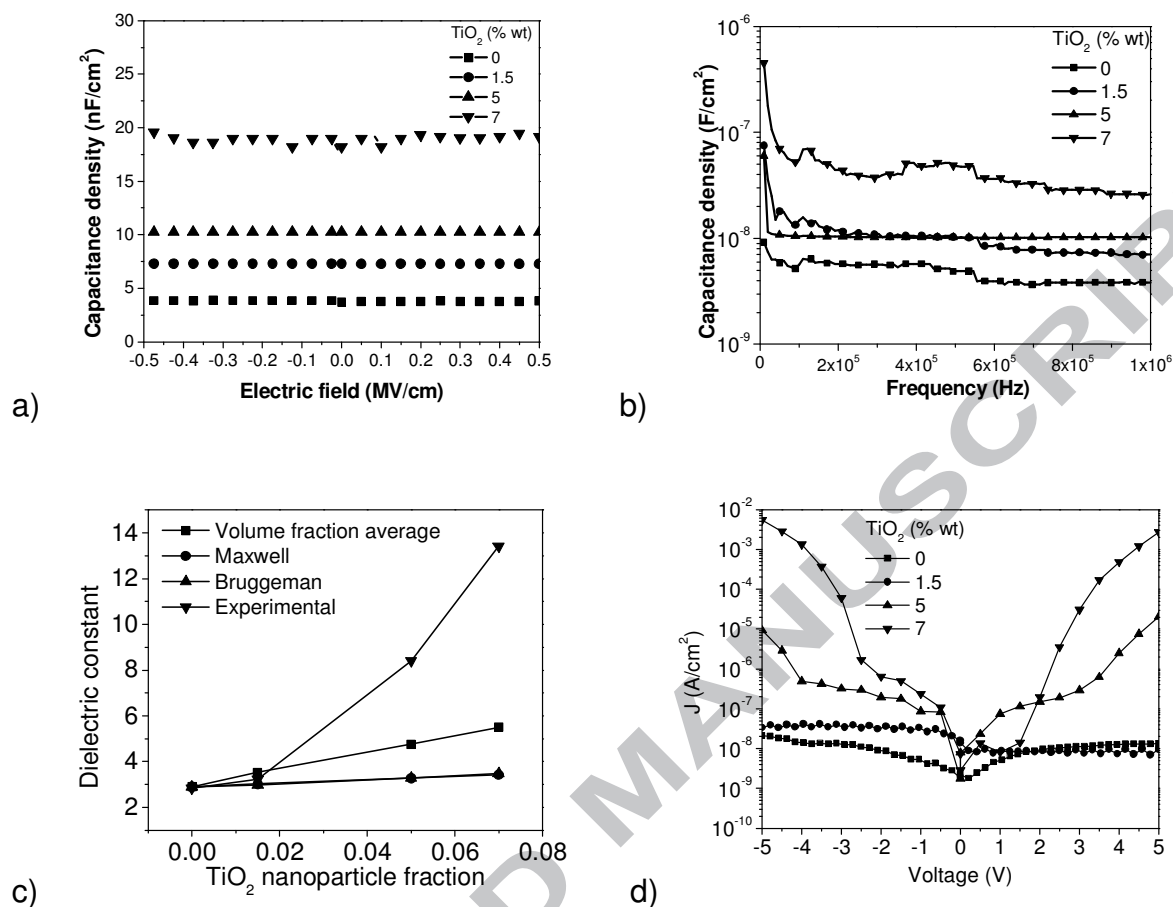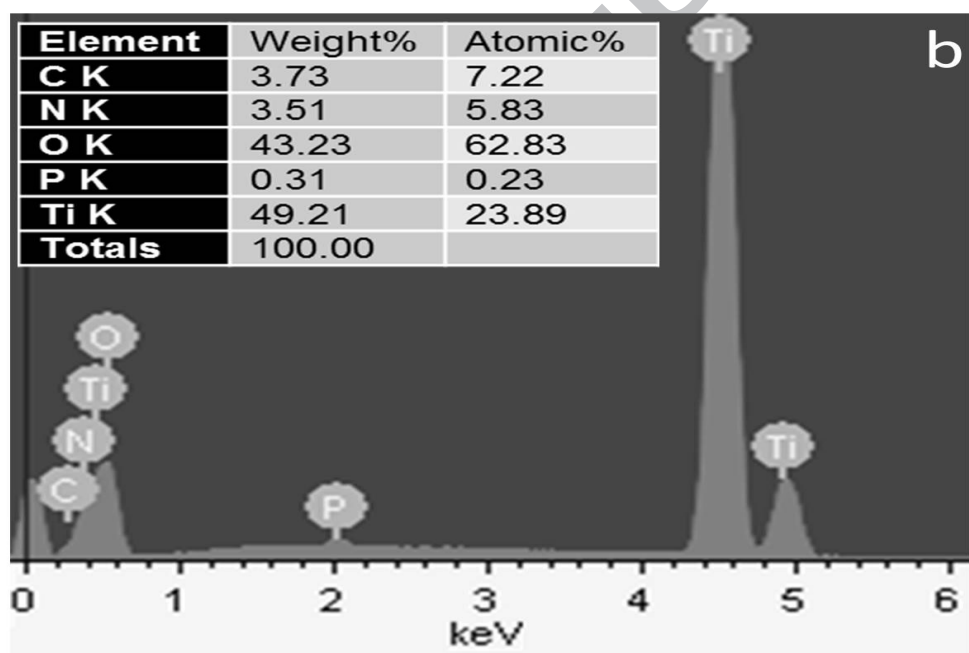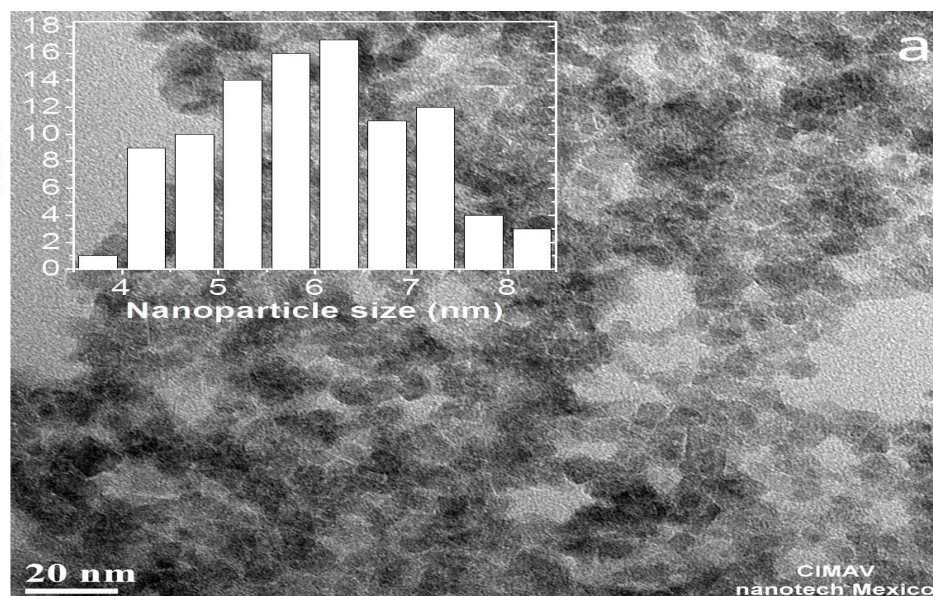| Element	Weight%	Atomic%
C K	3.73	7.22
N K	3.51	5.83
O K	43.23	62.83
P K	0.31	0.23
Ti K	49.21	23.89
Totals	100.00	

Figure 3.

Figure 4.

References.

1 G. Wang, D. Moses, A. Heeger, H. Zhang, M. Narasimhan, and R.J. Demaray, "Poly(3-hexylthiophene) field-effect transistors with high dielectric constant gate insulator", *J. Appl. Phys.,* vol. 95 no. 1, pp. 316-322, 2004.

2 L.A. Majewski, R. Schroeder, and M. Grell, "Low-Voltage, High-Performance Organic Field-Effect Transistors with an Ultra-Thin TiO2 Layer as Gate Insulator", *Adv. Mater.*, vol 15, no. 6 pp. 1017-1022, 2005.

3 Y. Jang, D.H. Kim, Y.D. Park, J.H. Cho, M. Hwang, and K. Cho, "Influence of the dielectric constant of a polyvinyl phenol insulator on the field-effect mobility of a pentacene-based thin-film transistor", *Appl. Phys. Lett.*, vol. 8, no. 15, pp. 152105–152105-3, 2005.

4 C. Stefan, I. Sava, V. Musteata, and M. Bruma. "Dielectric and conduction properties of polyimide films", *In Semiconductor Conference (CAS)* IEEE, vol. 2, pp. 253-256, 2011.

5 I. Mejia, M. Estrada, "Characterization of Polymethyl Methacrylate (PMMA) Layers for OTFTs Gate Dielectric", in Proceedings of the 6th International Caribbean Conference on Devices, Circuits and Systems, pp. 375-377, April 2006.

6 Q. Zhang, S. Ochiai, G. Sawa, A. Ohashi, K. Kojima, Y. Uchida, and T Mizutani, "Copper Phthalocyanine TFT with a polycarbonate gate dielectric layer", *Journal of the vacuum society of Japan*, vol. 50, no. 3, pp. 155-157, 2007.

7 G.H. Kim, S.M. Yoon, C.A. Kim and K.S. Suh, "Electrical and Chemical Properties of Photo-Cross-Linked Polymeric Insulating Materials", *Jpn. J. Appl. Phys.*, vol. 44 no. 13, pp. 416-418, 2005.

8 R. Ortiz, A. Facchetti, and T.J. Marks. "High-k organic, inorganic, and hybrid dielectrics for low-voltage organic field-effect transistors", *J. Chem. Rev.*, vol. 110, no. 1, pp. 205-239, 2010.

9 9 D. Tan, and P. Irwin, Advances in Ceramics, Electric and Magnetic Ceramics, Bioceramics, Ceramics and Environment, Chapter 7 Polymer Based Nanodielectric Composites, C. Sikalidis, Eds., 2011. InTech, pp. 115-132.

10 R.R. Prakash, S. Pandiarajan, P. Venkatesh, and N. Kamaraj, "Performance analysis of PMMA-TiO2 nanocomposite dielectrics," in International Conference on Emerging Trends in Electrical and Computer Technology (ICETECT), pp.46-49, March 2011.

11 D. Ma, T.A. Hugener, R.W. Siegel, A. Christerson, E. Martensson, C. Onneby, and L. Schadler, "Influence of nanoparticle surface modification on the electrical behavior of polyethylene nanocomposites", *Nanotechnology*, vol. 16, no. 6, pp. 724-731, 2005.

12 I. Inkyo, Y. Tokunaga, T. Tahara, T. Iwaki, F. Iskandar, C. Hogan, and K. Okuyama. "Beads Mill-Assisted Synthesis of Poly Methyl Methacrylate (PMMA)-TiO2 Nanoparticle Composites". *Ind. Eng. Chem. Res.*, vol. 47, no. 8, pp. 2597-2604., 2008.

13 Z.R. Ismagilov, L.T. Tsykoza, N.V. Shikina, V.F. Zarytova, V.V. Zinoviev (deceased), and S.N. Zagrebelnyi, "Synthesis and stabilization of nano-sized titanium dioxide". *Russian Chemical Reviews*, vol.78, no. 9, pp. 873-885, 2009.

14 C. Fang-Chung, C. Chih-Wei, H. Jun, Y. Yang, and L. Jen-Lien, "Organic thin-film transistors with nanocomposite dielectric gate insulator" *Applied Physics Letters*, vol. 85, no. 15, pp. 3295-3297, 2004.

15 D. Koziej, F. Fischer, N. Kränzlin, W. Caseri, and M. Niederberger, "Nonaqueous TiO2 Nanoparticle Synthesis: a Versatile Basis for the Fabrication of Self-Supporting, Transparent, and UV-Absorbing Composite Films", ACS Applied Materials & Interfaces, vol. 1, no. 5, pp. 1097-1104, 2009.

16 C. Xiaobo, and S.S. Mao, "Synthesis of titanium dioxide (TiO2) nanomaterials", *Journal of nanoscience and nanotechnology*, vol. 6, no. 4 pp. 906-925, 2006.

17 K. Tomita, V. Petrykin, M. Kobayashi, M. Shiro, M. Yoshimura, and M. Kakihana, "A Water-Soluble Titanium Complex for the Selective Synthesis of Nanocrystalline Brookite, Rutile, and Anatase by a Hydrothermal Method". *Angew. Chem. Int. Ed.*, vol. 45, no. 15, pp. 2378 –2381, 2006.

18 K. Prasad, D.V. Pinjari, A.B. Pandit, and S.T. Mhaske, "Synthesis of titanium dioxide by ultrasound assisted sol–gel technique: Effect of amplitude (power density) variation", *Ultrasonics Sonochemistry*, vol. 17, no. 4, pp. 697-703, 2010.

19 C. Martínez-Pérez, P. E. García- Casillas, H. Camacho-Montes, and H. Monreal-Romero, "Preparation of Titanum dioxide nanostructures facilitated by of Poly-L-lysine peptide" *J. of Alloys Comp.*, vol. 434-435, pp. 820-822, 2007.

20 Z. Tang, N. A. Kotov, "One-Dimensional Assemblies of Nanoparticles: Preparation, Properties, and Promise", *Adv. Mater.*, vol. 17, no. 63, pp. 951-962, 2005.

21 A. Cai, Y. Wang, L. Du, and Z. Ma, "DNA-templated apple-like cuprous oxide", *Mater. Lett.*, vol. 70, no. 1. pp. 149-151, 2012.

22 M. Di Ventra and M. Zwolak, "DNA Electronics", Enciclopedia of Nanoscience and Nanotechnology, vol 2, pp. 475-493

23 E. Heckman, J. Grote, F. Hopkins, and P. Yaney, "Performance of an electro-optic waveguide modulator fabricated using a deoxyribonucleic-acid-based biopolymer", *Appl. Phys. Lett.*, vol. 89, no. 18, pp. 181116-3, 2006.

24 F-X. Schmid, "Biological Macromolecules: UV-visible Spectrophotometry", Enciclopedia of Life Sciences, Macmillan Publishers Ltd., Chichester. 2001, pp 1-4.

25 M. Hamadanian, A. Reisi-Vanani and A. Majedi, "Sol-Gel Preparation and Characterization of Co/TiO2 Nanoparticles: Application to the Degradation of Methyl Orange", *J. Iran. Chem. Soc.*, vol. 7, no. 1, pp. 52-58, 2010.

26 S. Valencia, J.M. Marín and G. Restrepo, "Study of the Bandgap of Synthesized Titanium Dioxide Nanoparticules Using the Sol-Gel Method and a hydrothermal Treatment". *The Open Materials Science Journal*, vol. 4, no. 1, pp. 9-14, 2010.

27 S.Y. Baek, S.Y. Chai, K.S. Hur, and W.I. Lee, "Synthesis of Highly Soluble TiO2 Nanoparticle with Narrow Size Distribution", *Bull. Korean Chem. Soc.*, vol. 6, no. 9, pp. 1333-1334, 2005.

28 F.R. Keene, J.A. Smith, and J.G. Collins, "Metal complexes as structure-selective binding agents for nucleic acids", *Coordination Chemistry Reviews*, vol. 253, no. 15–16, pp. 2021-2035, 2009.

29 R. Caruso, M. Giersig, F. Willig and M. Antonietti, "Porous "coral-like" TiO2 structures produced by templating polymers gels", *Langmuir*, vol. 14, no. 22, pp. 6333–6336, 1998.

30 F. Saylikan, M. Asilturk, H. Sayilkan, Y. Onal, M. Akarsu, and E. Arpac, "Characterization of TiO2 synthesized in alcohol by a sol–gel process, The effect of annealing temperature and acid catalyst", *Turk. J. Chem.*, vol. 29, pp. 697–706, 2005.

31 E.F. Kaelble, Handbook of X-rays, McGraw –Hill, New York, 1967.

32 A.M. Tonejc, I. Djerdj, and A. Tonejc, "An analysis of evolution of grain size-lattice parameters dependence in nanocrystalline TiO2 anatase", *Materials Science and Engineering: C*, vol. 19, no. 1–2, pp. 85-89, 2002.

33 D.U. Lee, S.R. Jang, R. Vittal, J. Lee, and K.J. Kim, "CTAB facilitated spherical rutile TiO2 particles and their advantage in a dye-sensitized solar cell", *Solar Energy*, vol. 82, no. 11, pp. 1042-1048, 2008.

34 J.G.Hyun, S. Lee, S.D. Cho and K.W. Paik, "Frequency and Temperature Dependence of Dielectric Constant of Epoxy/BaTiO3 Composite Embedded Capacitor Films (ECFs) for Organic Substrate" in Proceedings of Electronic Components and Technology Conference, IEEE, pp. 1241-1247, 2005

35 T. Homma, "Low dielectric constant materials and methods for interlayer dielectric films in ultralarge-scale integrated circuit multilevel interconnections", *Materials Science and Engineering: R*, vol. 23, no. 6, pp. 243-285, 1998.

36 J. Kim, S.H. Kim, and Y.S. Kim, "Solution-Based TiO2-polymer Composite Dielectric for Low Operating Voltage OTFTs", *J. Am. Chem. Soc.*, vol. 132, no. 42, pp. 14721-14723, 2010.

37 S.D. Cho, J.Y. Lee, and K.W. Paik, "Effects of particle size on dielectric constant and leakage current of epoxy/barium titanate (BaTiO3) composite films for embedded capacitors", Advances in Electronic Materials and Packaging, EMAP, pp.63-68, 2001.

38 L. Yu, S. Ke, Y. Zhang, B. Shen, A. Zhang and H. Huang, "Dielectric relaxations of high-k poly(butylene succinate) based all-organic nanocomposite films for capacitor applications", *Journal of Materials Research*, vol. 26, no. 19, pp. 2493-2502., 2011.

39 P. Barber, S. Balasubramanian, Y. Anguchamy, S. Gong, A. Wibowo, H. Gao, H.J. Ploehn, and H.C. Loye, "Polymer composite and nanocomposite dielectric materials for pulse power energy storage", *Materials*, vol. 2, no. 4, pp 1697-1733, 2009.

40 S. Ge, Z. Ning, Z. "Dong and M. Shen, Investigation on dielectric properties of polycrystalline BT/ST multilayer thin films", Journal of Physics D: Applied Physics, vol. 35 no. 9, pp 906-909, 2002.

Element	Weight%	Atomic%
C K	3.73	7.22
N K	3.51	5.83
O K	43.23	62.83
P K	0.31	0.23
Ti K	49.21	23.89
Totals	100.00	

Research highlights

Synthesis of Titanium Oxide Nanoparticles Using DNA-Complex as Template for Solution- Processable Hybrid Dielectric Composites.

- We developed a modified synthesis method to produce titanium dioxide nanoparticles using a DNA complex at room temperature by the controlled hydrolysis of titanium isopropoxide.
- The nanoparticles presented anatase phase and were ~6 nm diameter with narrow size, stable in alcoholic solutions.
- Prepared composites reached a dielectric constant of 13.43 with 7 wt% of TiO_2, which was around 4.6 times larger than that of the pristine polycarbonate, more than the calculated by any of the used models.
- Maximum processing temperature was 90 °C, which enables their use in low-voltage, low-cost, flexible electronics.